electronics

MDPI

Article

Performance Evaluation of Directional Antennas in ZigBee Networks under NLOS Propagation Conditions

Joaquim Amândio Azevedo * and Filipe Edgar Santos

Center for Research in Mathematics and Applications (CIMA), Faculty of Exact Sciences and Engineering, University of Madeira, 9020-105 Funchal, Portugal; fsantos@uma.pt

* Correspondence: joaquimr@staff.uma.pt

Abstract: Many authors suggest directional antennas to enhance the transmission performance of ZigBee networks. For line-of-sight propagation, directional antennas can extend the transmission range or reduce the transmit power. Directional antennas may also reduce interference between networks operating in the same frequency channel. However, these antennas may not perform similarly under non-line-of-sight propagation conditions. This work presents a study with ZigBee modules comparing the performance of a directional antenna with an omnidirectional one. The measurements were conducted on a university campus for different propagation outdoor environments. A deconvolution technique was applied to estimate the received signal as a function of the azimuth angle. The results demonstrated that the received power followed the gain difference between antennas only for paths with low attenuation. Considering the same Effective Isotropic Radiated Power (EIRP), the system with directional antennas started to lose packets at the same distance as the omnidirectional antennas. The directional antenna did not allow the increase in the link range compared to the omnidirectional antenna. The power consumption was also measured for different transmit power levels of the ZigBee radio. The study showed that the control circuits of directional antennas typically consume more power than omnidirectional antennas operating at a higher transmit power level.

Keywords: radio wave propagation; channel measurements; directional antennas; wireless sensor networks; deconvolution technique

Citation: Azevedo, J.A.; Santos, F.E. Performance Evaluation of Directional Antennas in ZigBee Networks under NLOS Propagation Conditions. *Electronics* **2022**, *11*, 2032. https://doi.org/10.3390/electronics11132032

Academic Editor: Andrea Randazzo

Received: 2 June 2022
Accepted: 27 June 2022
Published: 28 June 2022

1. Introduction

Typically, omnidirectional antennas are preferred in wireless sensor networks (WSNs) because of their small size, low cost, easy deployment, and low complexity. However, many authors have recently defended the use of directional antennas. Directional antennas provide energy-saving or an extended transmission range, reduce collisions and interference, and can improve security against malicious attacks [1–4].

Regarding energy-saving, directional antennas may reduce the transmission power for the same EIRP. According to a work of Prayati et al. [5] with Telos B sensor nodes, the receive and listen operations consume more power than the transmission operation does. For a 114-byte packet, the active period lasted about 16 ms to transmit the packet. The transmission required three parts. The first part was the preparation of the packet and the transmission to the radio chip buffer, which used 24% of the total time. The second part was the back-off timeout with the duration dependent on the actual Carrier-Sense Multiple Access (CSMA) parameters, which used 54% of the total time. The last part was the transmission of the packet via the wireless radio, using 22% of the total time. The average current consumptions were 21.7 mA and 23.4 mA for the transmit powers of −10 dBm and 0 dBm, respectively. Catarinucci et al. [6] obtained the same conclusions in a study with the STM32W-EXT sensor node for two different transmit powers. For a sampling period of 100 ms, the average current consumptions were 21.4 mA and 21.2 mA

for the transmit powers of 3 dBm and −3 dBm, respectively. Piyare and Lee [7] studied the performance of ZigBee networks based on XBee S2 modules. The active period also consisted of three time intervals. The activation and deactivation lasted 20 ms (8.1 mA), the listening and receiving ACK packets lasted 6 ms (40 mA), and the transmission of a 111-byte packet lasted 3.6 ms (38 mA). The radios could operate with an output power between −8 dBm (boost mode disabled) and +3 dBm (boost mode enabled). The authors did not show the power consumption for the different transmit powers. According to the component's datasheet, the current consumptions were 35 mA and 40 mA for the boost modes disabled and enabled, respectively. The average current consumption of the active period was 17.8 mA for the first mode and 18.4 mA for the second mode.

As noted, reducing the transmit power lowers the power consumption of the sensor node. This conclusion has led several authors to propose the reduction in transmission power by using directional antennas [8–10]. In applications with directional antennas, the beam is oriented in the proper direction to increase the received power level. Beam control can be mechanical or electronic, but an electronically steerable beam is preferred [11]. Nevertheless, it should be considered that beam control in directional antennas also consumes energy. For instance, the typical control of reconfigurable antennas with PIN diodes requires a current of at least three milliamperes [12].

Directional antennas can also reject interference caused by multiple transmission technologies sharing the same channel. Staniec and Debita [13] indicated that directional antennas may remarkably improve the transmission performance of a sensor node. However, the work assumed sensor nodes deployed in an open area. Other works studied the application of directional antennas in WSNs, but they obtained the performance results by simulation [14,15]. Giorgetti et al. [16] studied the interference of the IEEE 802.11 g system in IEEE 802.15.4 sensor nodes. The beam selection with a four-beam patch antenna provided a higher Received Signal Strength Indicator (RSSI) when compared with the omnidirectional antenna. Nevertheless, the Wi-Fi source was close to the sink node.

Lin et al. [17] found that the correlation between RSSI and transmit power is approximately linear for different propagation environments. This correlation is not correct for the gain of the transmit antenna. Measurements carried out in zones with vegetation demonstrated that the power received by directional antennas was much lower than that obtained by an omnidirectional one for the receiver oriented to the transmitter. [18]. The best antenna orientation leading to the highest received signal may vary over time, particularly under Non-Line-Of-Sight (NLOS) conditions [19]. Michalopoulou et al. [20] investigated WSN performance using directional antennas in an outdoor environment through measurements. The experiments included zones with trees, traffic, and moving people. They concluded that the transmit power could be decreased by several dB when using directional antennas. However, the outdoor environment considered in the experiments had a path loss exponent of α = 2.41 and PL(1 m) = 40.28, which is close to the free-space conditions (α = 2, PL(1 m) = 40.1). Directional antennas require proper Medium Access Control (MAC) protocols, and routing is more complex [21,22]. Furthermore, most works consider the communication range of directional antennas modelled as a sector because of the complexity of a communication range derived from an actual directional antenna [23]. As WSN applications require compact systems, new directional antennas have been developed [24–33].

Many studies on the use of directional antennas in WSNs are theoretical. The few measurement results have demonstrated that directional antennas can effectively reduce the transmit power for the same range and minimize interference in LOS propagation. Although higher-gain antennas may provide more received power, it is necessary to evaluate how directional antennas behave in environments with attenuation. In these situations, signal transmission is strongly affected by the multipath phenomenon. Therefore, although a directional antenna increases the received signal in a given direction, the number of received reflections is reduced due to its narrower beam. In this work, the performance of directional antennas was compared to omnidirectional antennas in a ZigBee network

under NLOS propagation conditions. For the study, measurements were performed in environments affected by Wi-Fi and other ZigBee networks. The performance evaluation considered the RSSI and the Packet Delivery Rate (PDR) parameters. A deconvolution method was applied to estimate the signal distribution around the receiving antenna. These results aim to evaluate the effect of the environment on the received power for different radiation patterns.

2. Materials and Methods

2.1. Measurement Locations

The experiments with antennas considered three locations to evaluate different situations of NLOS propagation. The measurements were made on a university campus where several technologies transmit signals in the same frequency band of the ZigBee network.

The first location for channel measurements was the terrace of the University of Madeira, represented in Figure 1a. Figure 1b shows the site plan. The transmitter was placed inside a room on the floor below the terrace, 20 cm away from a wall. The environment was strongly affected by the Wi-Fi network and another ZigBee network used for monitoring purposes. We used six positions to measure the received power, marked in the figure by numbered circles.

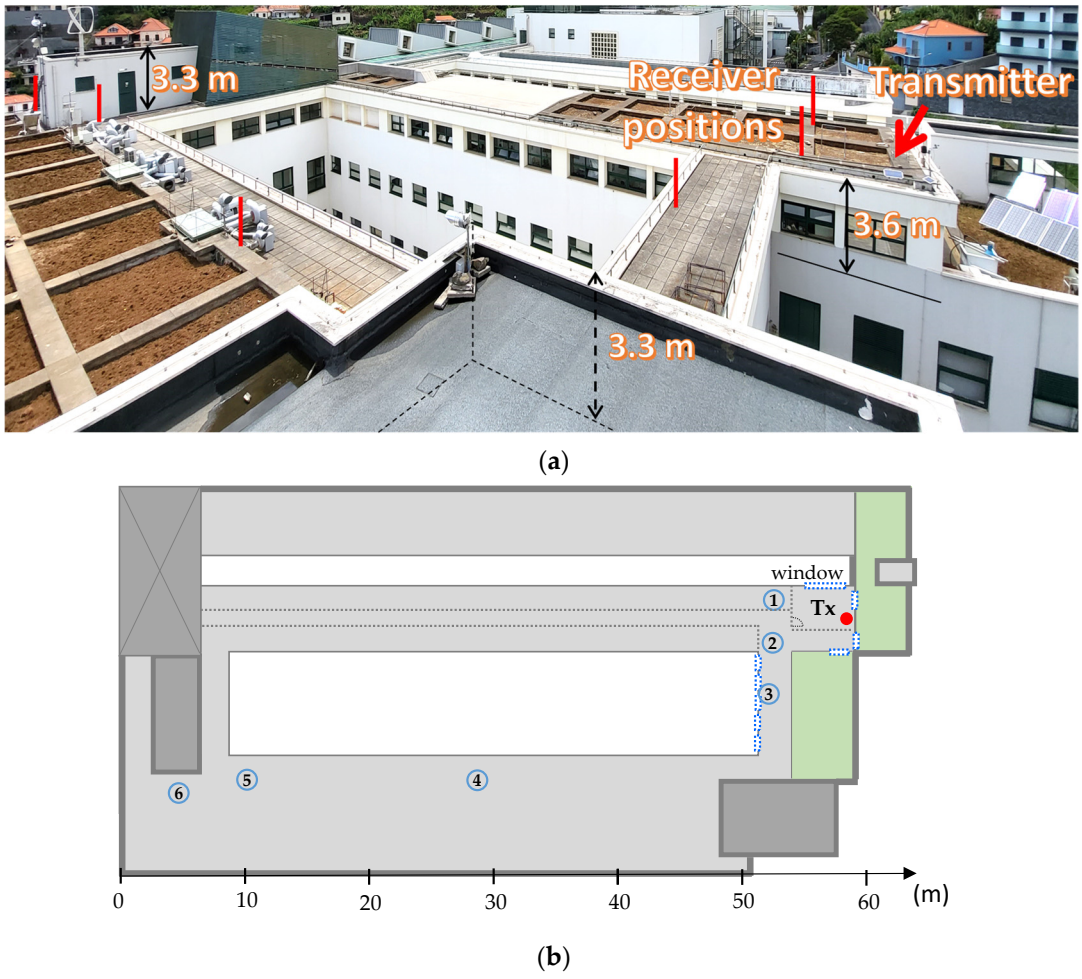

Figure 1. Location 1—terrace of the University of Madeira: (**a**) image of the location; (**b**) plan with the transmitter and receiver positions.

The second location was the environment around the university building, as shown in Figure 2a. This figure also shows some measurement positions. A street surrounds the building, and a wall is on the opposite side. Figure 2b represents the site plan with the

receiver positions used for the measurements. For position 1, we oriented the receiver toward the transmitter. In this case, the transmission occurred in the line-of-sight. In the other cases, the building blocked the direct signal, and the received power was mainly due to reflections and diffraction of the transmitted signal. The distance between the transmitter and the last receiver position was 95 m.

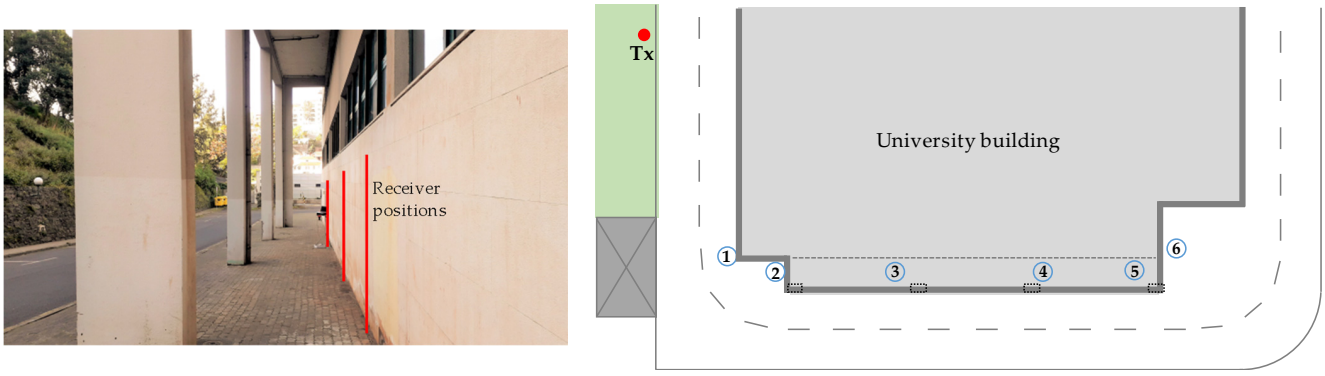

(**a**) (**b**)

Figure 2. Location 2—street around the building: (**a**) image of the location; (**b**) plan with the transmitter and receiver positions.

The third location was a zone with dense vegetation on the university campus, as shown in Figure 3a. Figure 3b represents the site plan. We performed measurements between 20 m and 110 m from the transmitter. The Wi-Fi network also affected the transmissions. For some measurement positions, the building was visible from the receiver.

(**a**) (**b**)

Figure 3. Location 3—vegetation zone: (**a**) image of the location; (**b**) site plan.

2.2. Experimental Setup

We used XBee S2C modules from Digi [34] in the experimental setup of the work. These ZigBee sensor nodes operate in the Industrial, Scientific, and Medical (ISM) band of 2.4 GHz. The maximum EIRP allowed in Europe for this band is 10 dBm. The transmit power levels of the XBee S2C are between –5 dBm and +5 dBm. A boost mode allows a maximum power of 8 dBm. The receiver sensitivity is −100 dBm with boost mode disabled, and −102 dBm with boost mode enabled. The datasheet shows a transmit current of 33 mA @ 3.3 V with boost mode disabled (45 mA—boost mode enabled), receive and idle currents of 28 mA (31 mA—boost mode enabled), and a sleep mode current below 1 µA. The data rate was 250 kbit/s.

The transmitter was implemented with an Arduino Pro mini microcontroller and an XBee module programmed as a router. An 1800 mAh @ 3.7 V lithium battery was used as a power supply. The system transmitted packets of 40 bytes at a rate of one per second. We numbered the packets to estimate the PDR parameter. The receiver was implemented with an XBee module, programmed as a coordinator, and connected to a personal computer. We utilized the XCTU software from Digi [34] to record the packets and extract the RSSI value of the last received packet. The antennas employed were 2 dBi monopoles [35] and 9.5 dBi suspended patches as omnidirectional and directional antennas, respectively. We chose the patch antenna because of its compact size (10 cm $\times$ 10 cm) and high gain. The transmitter and receiver used the same type of antenna because a sensor node must operate in both modes in practical situations. These antennas were mounted on 2.5 m high poles. The poles allowed rotation to determine the maximum received power of the directional antennas. The antennas operated in vertical polarization.

2.3. Extraction of the Received Signal

In NLOS environments, the power received by an antenna can be mainly due to reflections and other propagation phenomena. Knowing the distribution of the input signal at the receiver as a function of the azimuth angle allows us to evaluate the main directions in space that contribute to the received power. Cui et al. [36] developed a method applied to vegetation to determine the density of the transmitted power just before reaching the receiver antenna. We used this procedure in the environments described in Section 2.1 to obtain the signal distribution at the receiving antenna input. The technique assumed that the scattered wave trains are uncorrelated in phase. Thus, the power can be summed at the receiver in real quantities. Measuring the signal distribution requires a very-high-gain antenna. The problem with this procedure is related to the antenna radiation diagram because it is not an ideal pulse.

Considering $i(\theta)$ as the directional intensity of the incoming signal as a function of the azimuth angle θ and $g(\theta)$ as the radiation pattern of the receiver antenna, the measured power is given by a convolution:

$$p(\theta) = g(\theta) * \ i(\theta) \tag{1}$$

where $*$ represents the convolution operation. The Fourier Transform is

$$P(\omega) = G(\omega)I(\omega) \tag{2}$$

Knowing $G(\omega)$, $I(\omega)$ can be extracted by deconvolution. However, very high errors may occur when $I(\omega)$ is determined from $P(\omega)/G(\omega)$ because of the division by values close to zero. Following the technique proposed in [36], a better estimate of $I(\omega)$ can be given by

$$I_e(\omega) = P(\omega)\frac{G^*(\omega)}{|G(\omega)|^2 + \lambda} \tag{3}$$

where * is the complex conjugate. The parameter λ was determined by evaluation of the following error function:

$$e(\theta) = p(\theta) \ - \ g(\theta) * \ i_e(\theta) \tag{4}$$

We evaluated the error in the frequency domain for simplicity. From Equation (3), there is no effect in the deconvolution error when λ is too low. On the other hand, the signal distortion is high if λ is too high [37]. A decision criterion was to choose a value of λ that produced a root mean square of the normalized error of 0.1.

The received power was measured as a function of the azimuth angle with an antenna of 17.5 dBi. This antenna consists of an array of 4 $\times$ 2 suspended patches. The radiation pattern of this antenna, $g(\theta)$, was measured inside an anechoic chamber, giving the result shown in Figure 4a. Figure 4b shows the radiation pattern of the directional antenna presented in the previous section.

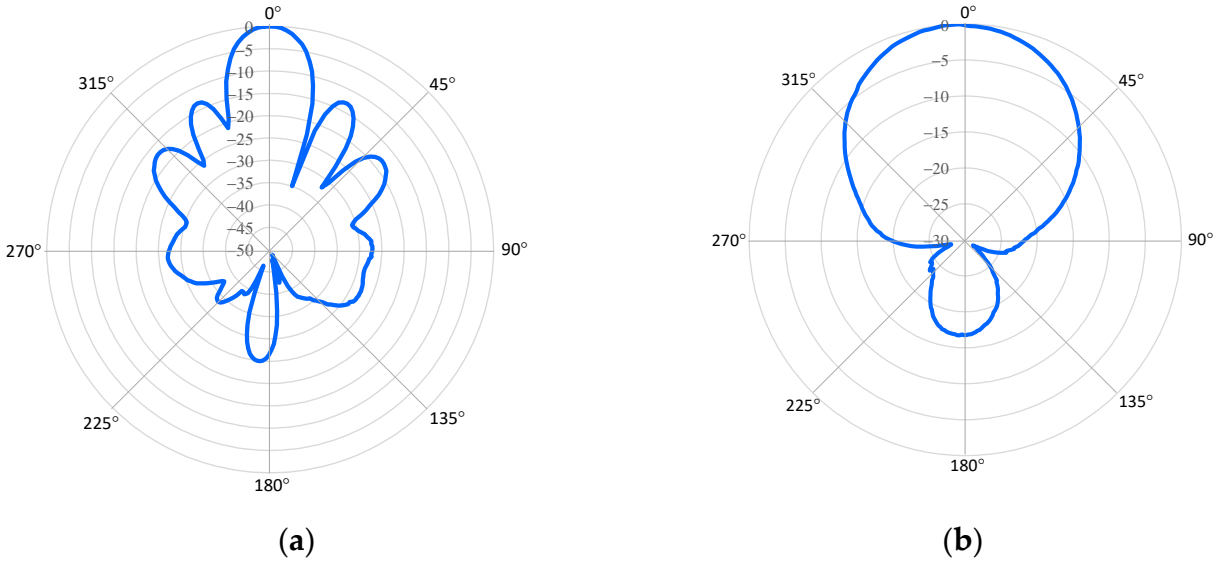

Figure 4. The radiation patterns: (**a**) 17.5 dBi gain antenna; (**b**) 9.5 dBi gain antenna.

We attached the receiving antenna of 17.5 dBi to a stepper motor mounted on a pole to measure the signal distribution. The transmitter consisted of a radio-frequency generator connected to the antenna. We used the Lab Brick Signal Generator from Vaunix Technology Corporation [38], model LSG-602. This generator allows the transmission of a signal between 1500 MHz and 6000 MHz, with an output power between −45 dBm and 10 dBm. We used the spectrum analyzer FSH8 from Rohde and Schwarz [39] connected to the 17.5 dBi gain antenna as a receiver. The received power was recorded on a personal computer connected to the spectrum analyzer. The bandwidth considered in the measurements was 30 kHz. The system obtained about 300 samples in each complete rotation of the receiver antenna.

3. Results

Communications in typical wireless sensor networks are bidirectional. Therefore, the present study assumed that both sides of the communication link have similar conditions. In this way, the transmitter and the receiver used the same type of antenna during the experiments with XBee. Considering the maximum value of EIRP, the transmit powers of the systems with omnidirectional and directional antennas were +8 dBm and 0.5 dBm, respectively. The goal was to determine the maximum range in each environment for both cases. This objective considered that the sensing range is greater than the communication range in many practical NLOS transmission situations.

3.1. Location 1—Terrace

For location 1, we chose two types of orientation for the transmit directional antenna. The first was to orient the transmit antenna toward the room door, approximately in line with most receiver positions (Directional—orientation 1). In the second case, we pointed the transmit antenna in a direction that provides the highest average RSSI and PDR (Directional—orientation 2). In this situation, the antenna pointed to the window mentioned in Figure 1. We moved the receiving antenna during measurements within a radius of about 10 cm around the central position to obtain the average. For the directional antenna, we rotated the receiving antenna to find the highest average RSSI and PDR. In this case, orienting the antenna toward the building in front of the window provided the best results. We recorded about one hundred packets in each measurement session.

Figure 5 shows the average RSSI as a function of the distance to the transmitter for the three studied situations. The labels inserted in the graph relate the distance with the receiver position shown in Figure 1b. The expected values of received power under free-

space conditions are also represented in Figure 5a to determine the attenuation introduced by the medium. This attenuation was almost constant except for distances close to the transmitter. The high attenuation was due to the structure of the building. The directional antenna—orientation 2—provided the highest average RSSI values, with an average of 5 dB above the omnidirectional one. However, the expected received power under free-space conditions would be 7.5 dB higher. Despite the XBee sensitivity being −100 dBm, the lowest measured RSSI was −90 dBm because of the Wi-Fi interference. Figure 5b shows the PDR for the three situations. All antennas have similar results for the first four receiver positions. However, the directional antenna—orientation 2—lost some packets in the first positions because the antenna pointed directly to the Wi-Fi source. Above the fourth position, the directional antenna—orientation 1—had the lowest performance. The systems were not able to receive packets above the last point.

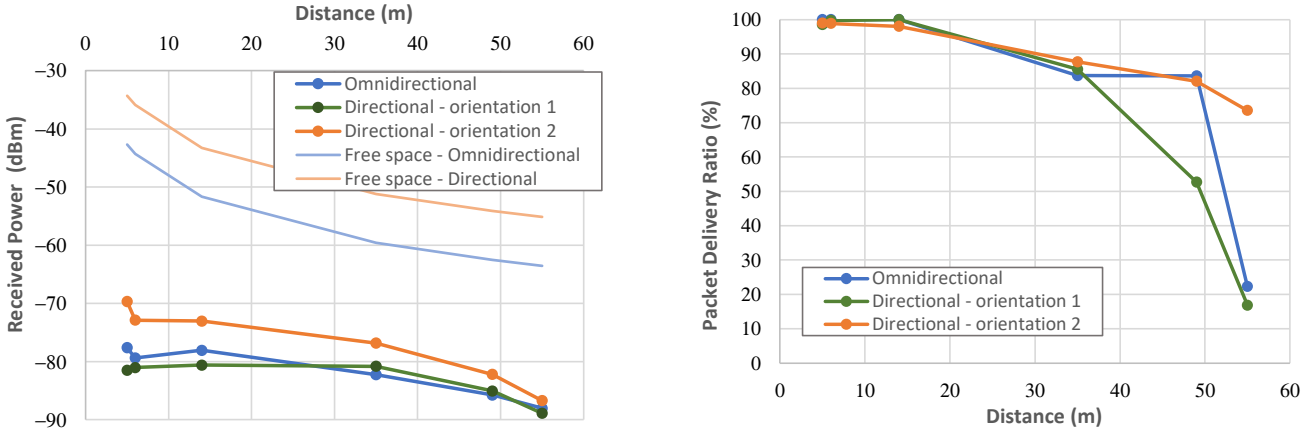

(**a**) (**b**)

Figure 5. Measurements results of XBee for location 1: (**a**) average RSSI; (**b**) PDR.

We also performed a set of measurements to assess the signal distribution around the receiver. The technique described in Section 2.3 allowed for extracting the received signal as a function of the azimuth angle. We used the transmitter's direction for the angle count, and the rotation was clockwise. Figure 6a shows the received power for position 2, and Figure 6b shows the received signal after removing the antenna radiation pattern effect. These results demonstrated that the highest components of the received signal were in the same direction as that obtained for the RSSI. However, the antenna received many signal reflections from other directions. The omnidirectional antenna spreads the transmitted power more in multiple directions. The received signal was lower for the directional antenna—orientation 1. In this case, we can observe in Figure 6a signal peaks for angles around −120 degrees. This result confirmed the Wi-Fi interference observed during measurements, which occurred as bursts of high signal levels.

The received signal also allowed the received power for each antenna to be estimated. For this, Equation (1) was employed with $g(\theta)$ as the radiation diagram of the respective antenna. Figure 7 shows the result for the directional antenna—orientation 2—in position 2. The estimated power level in the maximum direction was −80 dBm. Applying the procedure to the omnidirectional antenna gave an estimated power of 5 dB below the value of the directional antenna. Applying it to the case of the directional antenna—orientation 1—the estimated power was 10 dB below.

The received power was measured using the signal generator and the spectrum analyzer to evaluate the one estimated by the previous procedure. Table 1 shows the results for the six receiver positions.

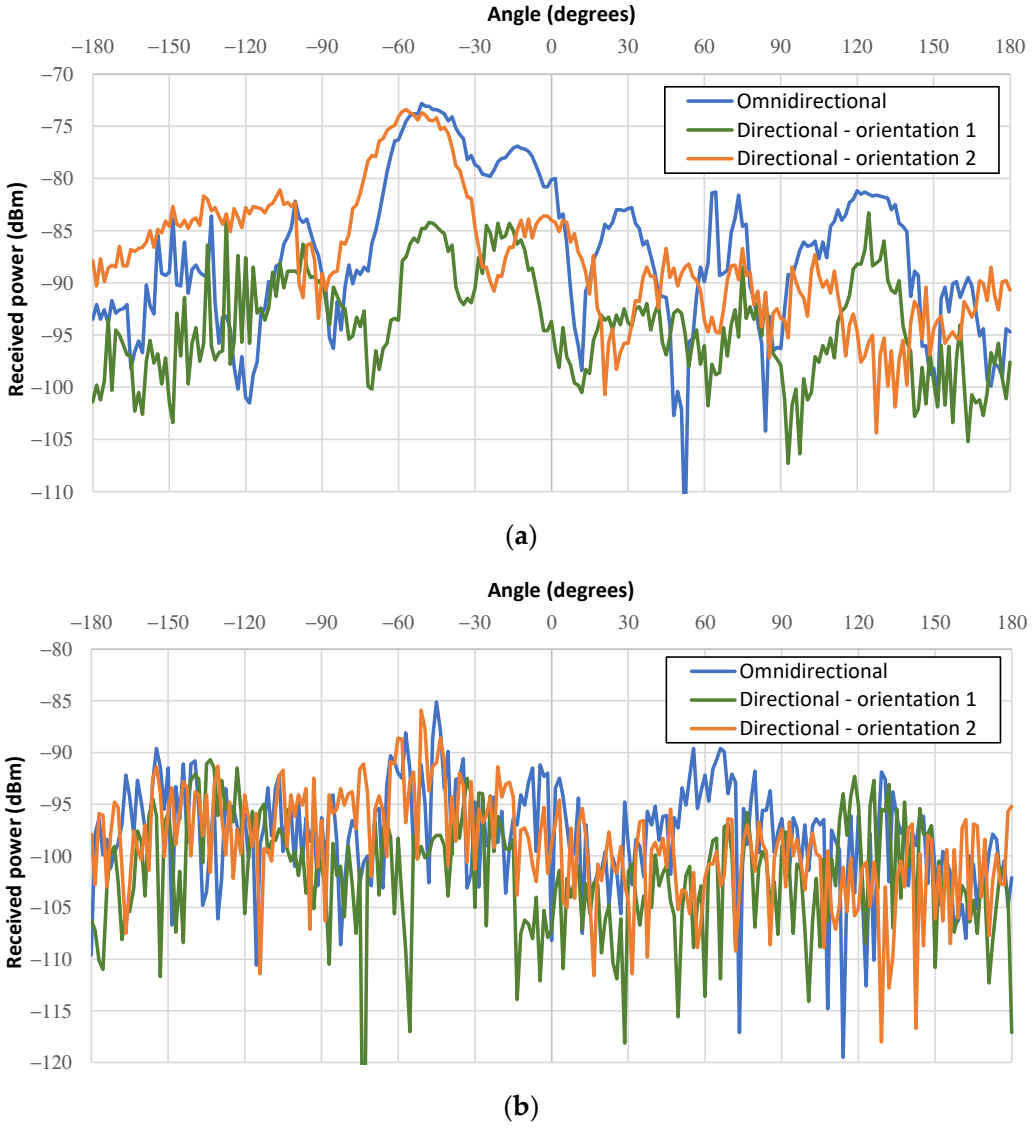

Figure 6. Measurements results with a signal generator: (**a**) received power; (**b**) received signal after deconvolution.

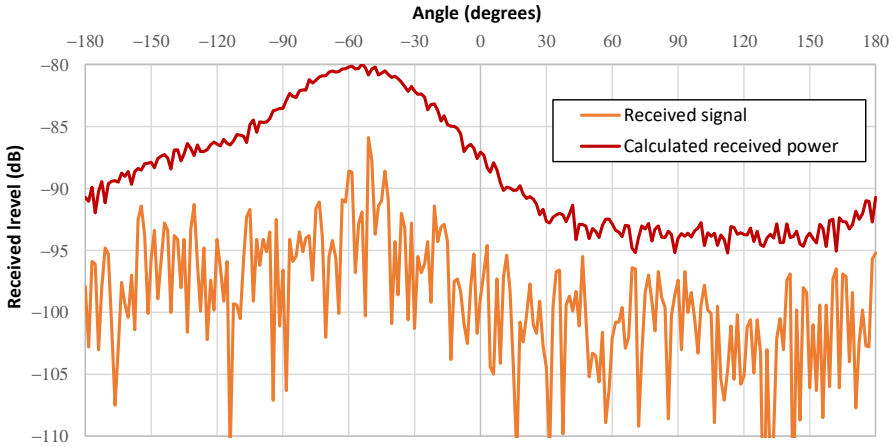

Figure 7. Calculated received power for the directional antenna—orientation 2.

Table 1. Measurement results.

	Omnidirectional		Directional—Orient. 1		Directional—Orient. 2	
Position	**RSSI (dBm)**	**P_s (dBm)**	**RSSI (dBm)**	**P_s (dBm)**	**RSSI (dBm)**	**P_s (dBm)**
1	−77.6	−80.9	−81.5	−85.0	−69.7	−74.1
2	−79.4	−82.8	−81.0	−84.6	−72.9	−76.2
3	−78.0	−81.2	−80.6	−85.1	−73.0	−76.8
4	−82.2	−85.8	−80.8	−85.5	−76.8	−79.9
5	−85.8	−89.9	−85.1	−91.0	−82.2	−86.5
6	−88.0	−93.4	−88.9	−95.6	−86.7	−92.5

The RSSI values are those represented in Figure 5a, and P_s is the received power from the generator. As we can observe, P_s was always below the RSSI because it corresponded to a received power of a narrowband signal. On the other hand, RSSI corresponded to the received signal plus noise and interference measured in the ZigBee bandwidth of about 2 MHz. Figure 8a shows the difference between the average power received by the directional antenna and the omnidirectional antenna. As can be seen, the results obtained by the generator followed those obtained by the XBee. Despite the higher gain of the directional antenna, the received power difference decreased with increasing distance to the transmitter. The power received by the directional antenna—orientation 1—was always below the power of the omnidirectional antenna. The estimated power was, on average, 3.6 dB below the measured power, with a standard deviation of 1.5 dB.

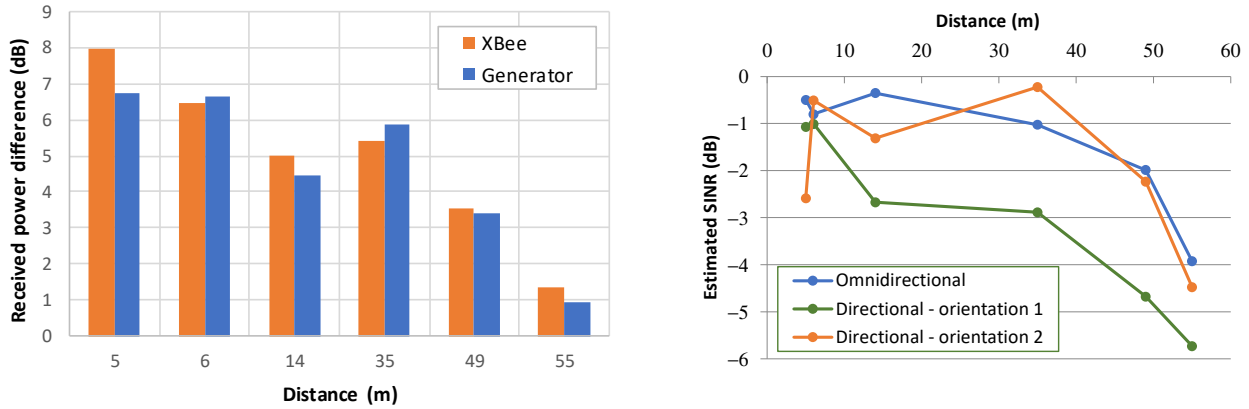

Figure 8. (**a**) Power difference between omnidirectional and directional antennas; (**b**) estimated SNIR.

Figure 8b shows the estimated Signal-to-Interference-plus-Noise Ratio (SINR). The received power is defined by

$$P_r = P_s + P_{ni} \tag{5}$$

where P_s is the received signal power and P_{ni} is the interference and noise power. With P_r determined from the RSSI and P_s approximated by the values presented in Table 1, the *SINR* was given by

$$SINR\ (\text{dB}) = 10\log_{10}\left(\frac{P_s}{P_{ni}}\right) = 10\log_{10}(P_s) - 10\log_{10}\left(10^{\frac{RSSI}{10}} - P_s\right) \tag{6}$$

From Figure 8b, the *SINR* was always negative due to Wi-Fi interference. The directional antenna—orientation 1—had the lowest *SINR* for almost all receiver positions. The *SINR* confirmed the high loss of packets for longer distances for the three antenna situations. These results also confirmed why the directional antenna could not increase the range compared to the omnidirectional one. Although the directional antenna had

an additional 7.5 dBi gain, the received power was only about 1 dB above that of the omnidirectional antenna.

3.2. Location 2—Street

The received power at location 2 was affected by the blockage caused by the building. Figure 9 shows the results of the average RSSI and the PDR obtained by the XBee system. As position 1 was under LOS conditions, the received signal was close to that of free space. In this case, the directional antenna had the highest received power when oriented toward the transmitter. For positions 2 to 5, the direction of this antenna was toward the street's curve. For position 6, the orientation was perpendicular to the building. Therefore, the wall of Figure 2a reflected the transmitted signal to the receiver. The directional antenna's average received power was 5.1 dB above the value of the omnidirectional one. However, the last position's average power difference was only 0.6 dB. Observing Figure 9b, the PDR was 100% for all receiver positions except the last one. This position was on the opposite side of the building, as observed in Figure 2b.

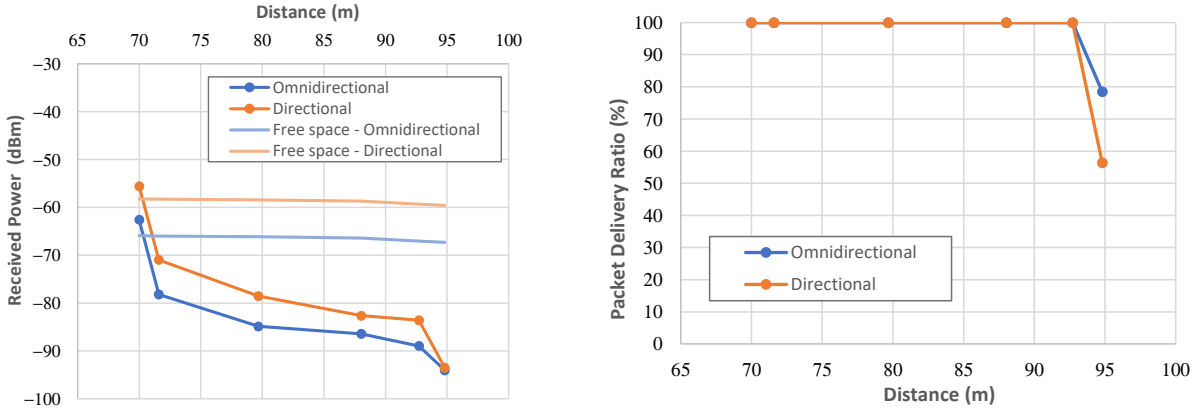

(**a**) (**b**)

Figure 9. Measurements results of XBee for location 2: (**a**) average RSSI; (**b**) PDR.

We also applied the deconvolution technique to estimate the received signal as a function of the azimuth angle. Figure 10 shows the results for two receiver positions. For position 4, the highest received signal came from a specific direction. This direction coincided with that used for the directional antenna to obtain maximum power. The signals received at position 6 were more dispersed in space, making the omnidirectional antenna more effective in capturing the transmitted power.

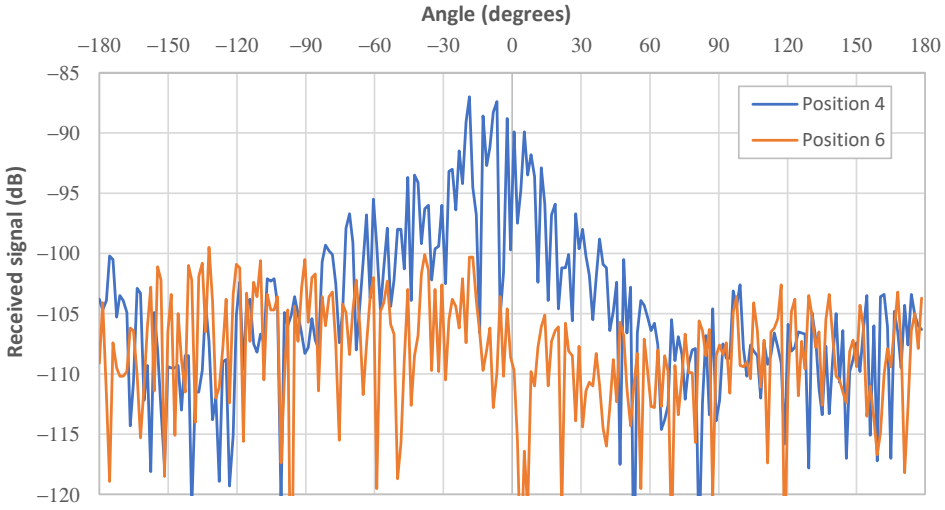

Figure 10. Received signal after deconvolution for two receiver positions.

3.3. Location 3—Vegetation

The third location for measurements was an area with vegetation. The Wi-Fi network broadcast from the university building also affected the ZigBee channel. Unlike the other environments, the signal attenuation was mainly due to obstruction in the entire propagation path. With the transmitter in a fixed position, we measured the RSSI and the PDR for the nine positions shown in Figure 3. The transmitter and receiver directional antennas were oriented to provide the highest RSSI and PDR values. We used the line formed by the transmitter and receiver antennas for the angle count. ϕ_T and ϕ_R are the angles of the transmitter and receiver antennas, respectively. For distances up to 70 m, both antennas were oriented in the same direction, meaning that $\phi_T = \phi_R = 0°$. For the other distances, we obtained $\phi_T = 30°$ and $\phi_R = -50°$, $\phi_T = 20°$ and $\phi_R = -40°$, $\phi_T = 0°$ and $\phi_R = -20°$, and $\phi_T = \phi_R = 0°$, for 80 m, 90 m, 100 m, and 110 m, respectively. The non-zero angles corresponded to rotating the antennas toward the university building. Figure 11 shows boxplots of the dispersion of the measured RSSI. The fading due to vegetation may introduce RSSI variations of 10 dB or 15 dB in a few cm.

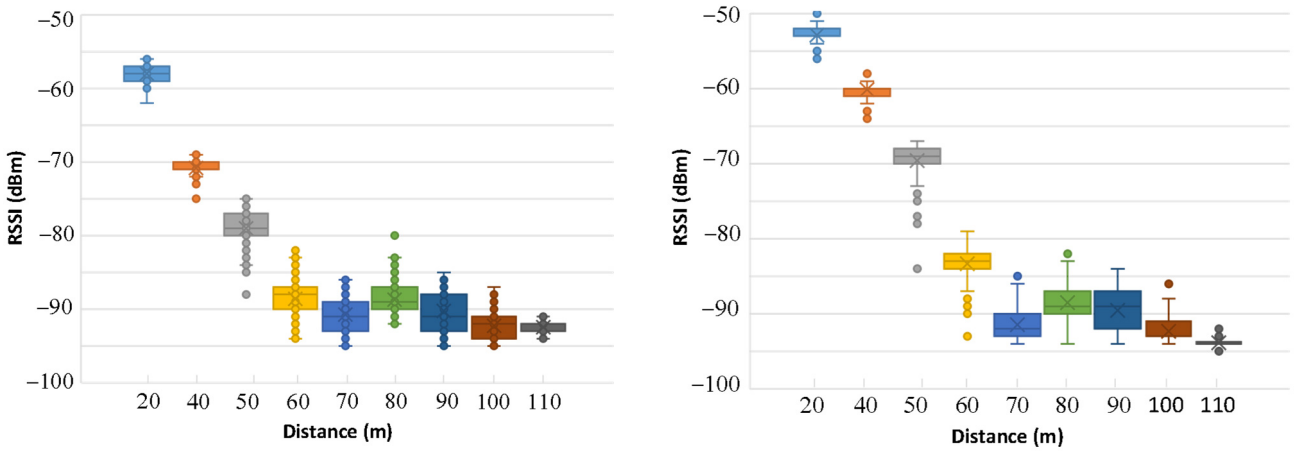

Figure 11. RSSI measurements: (**a**) omnidirectional antenna; (**b**) directional antenna.

Figure 12 shows the average RSSI and PDR. Regarding the RSSI, the directional antenna received, on average, 7.2 dB more power than the omnidirectional one for distances up to 60 m. Above this distance, the RSSI was almost the same for both antennas. The attenuation increased with distance because of the vegetation density. Compared to location 1, Wi-Fi caused less interference, so the lowest measured RSSI value was −95 dBm. Figure 12b shows the packet delivery ratio. The systems did not lose packets for distances up to 60 m. Above this distance, the packet loss was similar for both antennas. However, the directional antenna had 7.5 dBi more gain than the omnidirectional one.

To understand the degradation in the directional antenna performance compared to the omnidirectional one, we measured the received signal as a function of the azimuth angle. Figure 13a shows the results for the distance of 50 m. In this case, the higher components arrived at the receiver from the transmitter's direction, and the directional antenna provided a higher RSSI than the omnidirectional antenna. Figure 13b shows the results for the distance of 80 m. In this situation, the directional antenna did not improve the transmission performance compared to the omnidirectional one. For distances between 60 m and 100 m, the signal received by the system using omnidirectional antennas provided higher signal components for various azimuth angles, as seen in Figure 13b. The results for the directional antenna shown in Figure 13 also confirmed that the receiving antenna should be oriented around −50° to provide the highest received power. This orientation was the same as that for XBee to produce the best results. We noted that this coincided with the direction of the university building, which was the source of the Wi-Fi interference.

Figure 13c shows the results for the distance of 100 m. Observing Figure 12b, the receiver lost many packets above this distance. The signals represented in Figure 13c show that they were more dispersed in space. Once again, the system with the omnidirectional antennas provided higher received signal components for various angles.

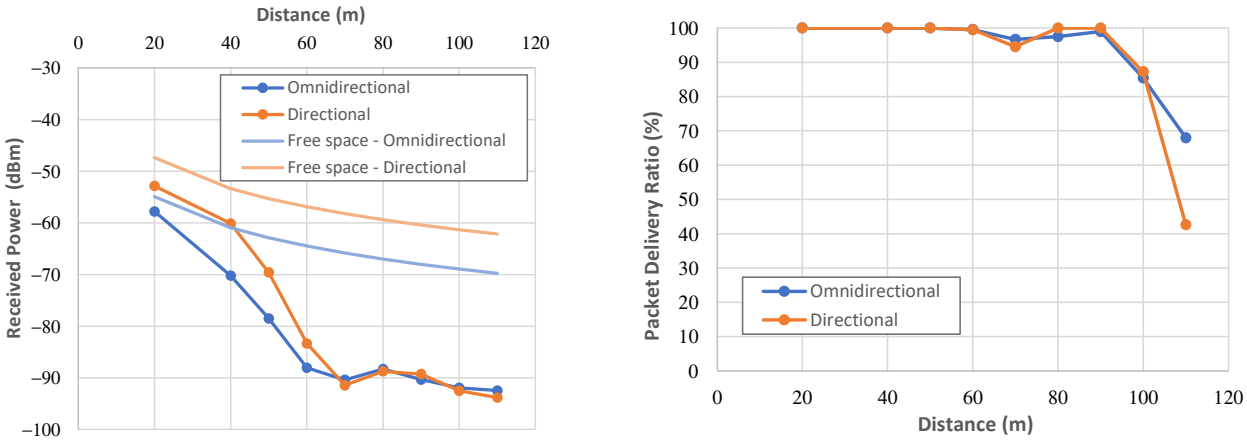

(**a**) (**b**)

Figure 12. Measurements results of XBee for location 3: (**a**) average RSSI; (**b**) PDR.

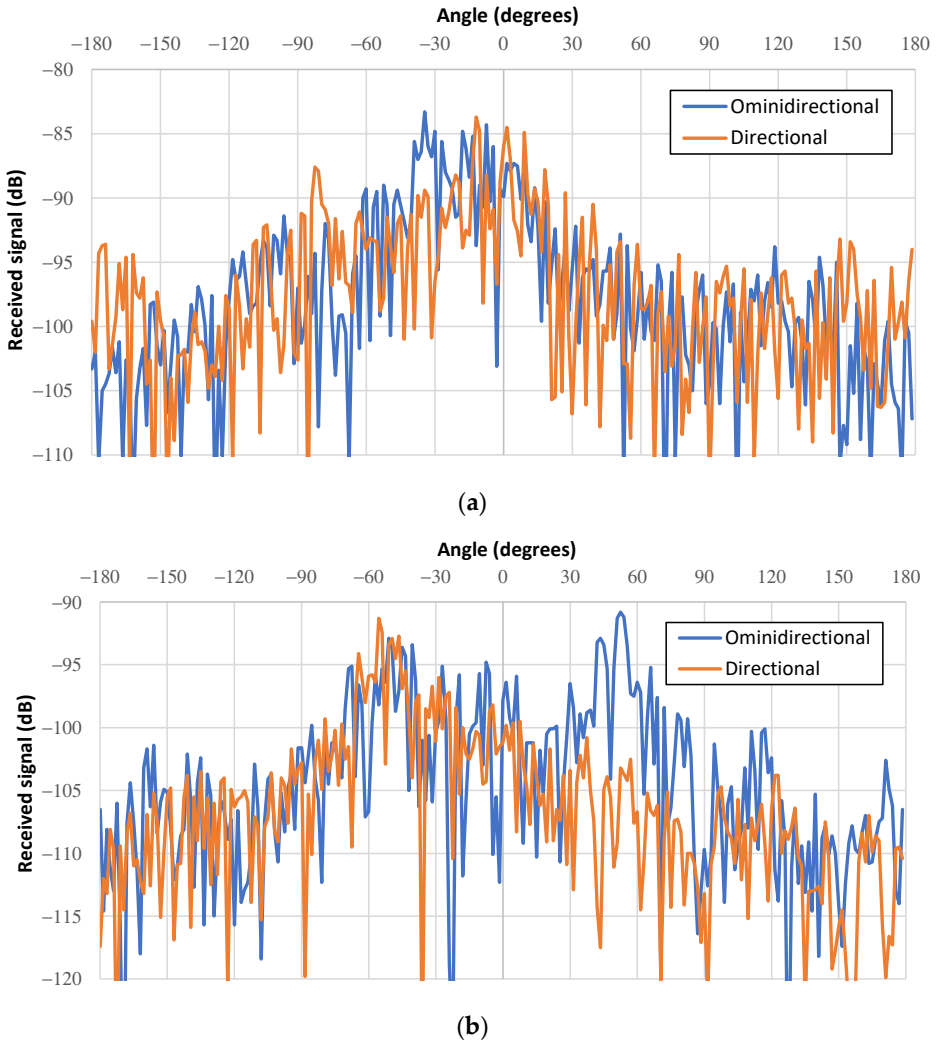

(**a**)

(**b**)

Figure 13. *Cont.*

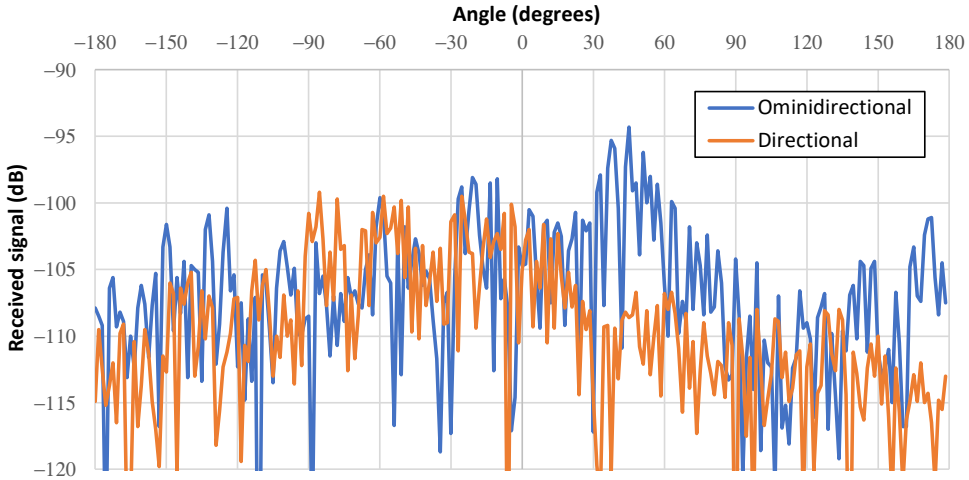

(**c**)

Figure 13. Received signal after deconvolution for different distances from the transmitter: (**a**) 50 m; (**b**) 80 m, (**c**) 100 m.

The signal distribution also allowed us to estimate the narrow-band received power. The received power was determined through Equation (1), with $g(\theta)$ being the radiation pattern of each receiver antenna. We addressed the quality of these estimates with auxiliary measurements. The mean difference between the measured and estimated values was 1.2 dB, and the standard deviation was 3.6 dB.

4. Discussion

The results indicate that directional antennas did not improve the performance of omnidirectional antennas under NLOS conditions. Several authors have proposed the use of directional antennas to suppress interference. The study carried out in the three zones showed that the directional antennas were oriented in the direction of the strongest signal to provide the best results, as expected. However, these signals often came from directions with high Wi-Fi interference.

The directional antenna used in this work can increase the link budget by 7.5 dB. This gain allows for double the range under conditions close to free space. The performance of the directional antenna was better when the received signal was more concentrated in a specific direction. On the other hand, when higher-signal components reached the receiving antenna from various directions, omnidirectional antennas had similar results to directional antennas. Furthermore, it is only feasible to control the receiving antenna to increase the received power in practical situations. Control of the transmitting antenna requires feedback from the receiver. However, there is no active communication link yet. Therefore, the performance of directional antennas can be lower than that described in this work.

In this study, the systems operated with the same EIRP. The reason for choosing this condition was to obtain the maximum range using the maximum transmit power allowed by the regulations. In this case, the transmit power of the directional antenna system was 7.5 dB below the transmit power of the omnidirectional antenna system. Under these conditions and for a PDR greater than 90%, the system range at location 1 was about 30 m. The reached distance for the systems at locations 2 and 3 was about 90 m.

The system with the omnidirectional antenna used a higher transmit power. Higher transmit power means more power consumption. That is why many authors have proposed directional antennas, as they can reduce the power consumption of battery-operated networks. However, the control of directional antennas also consumes energy. Therefore, a comparison of power consumption between systems is required. Considering the transmit power, we measured the current consumption of the XBee S2C by inserting a shunt resistor

of 1 Ω between the battery and the supply pin of the sensor node. The XBee S2C module uses the Silicon Labs EM357 chipset [34]. An oscilloscope connected to the resistor terminals allowed us to obtain the current results. Figure 14 shows the measured transmit current for each power level. There is a difference of 12 mA between the highest and the lowest power levels with the boost mode disabled. Activating the boost increased the current consumption, on average, by 5.5 mA.

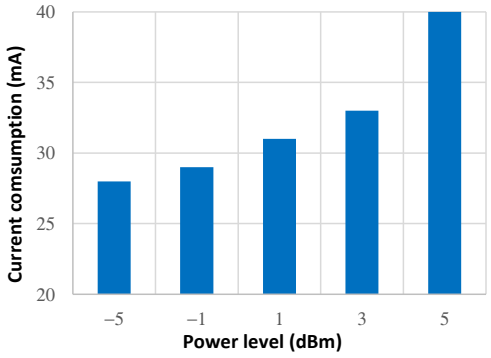

Figure 14. Current consumption of the XBee S2C.

We measured the current consumption with the XBee operating as an end device and transmitting 111-byte packets. Figure 15 shows the current consumption for the highest power level and two operating conditions. The graphs are similar to those represented in [40] for the radio CC2530. Figure 15a refers to the case in which the system uses application acknowledgements (ACK). In this case, the active period lasted 98.5 ms. The duration of the transmit mode and the idle/receive modes were 3.6 ms and 5.7 ms, respectively. For a processing current of 9 mA, the system consumed, on average, 11.6 mA during the active period. The current consumption would be 11 mA for the lowest transmit power level. The difference between both cases was 0.6 mA (1 mA with boost mode enabled). Figure 15b describes the current consumption for transmissions without application acknowledgements. The active period lasted 18.6 ms. The difference in current consumption between the highest and lowest transmit levels was, on average, 2.3 mA (3.5 mA with boost mode enabled). When the sensor node operates as a router, the power consumption is practically independent of the transmit power.

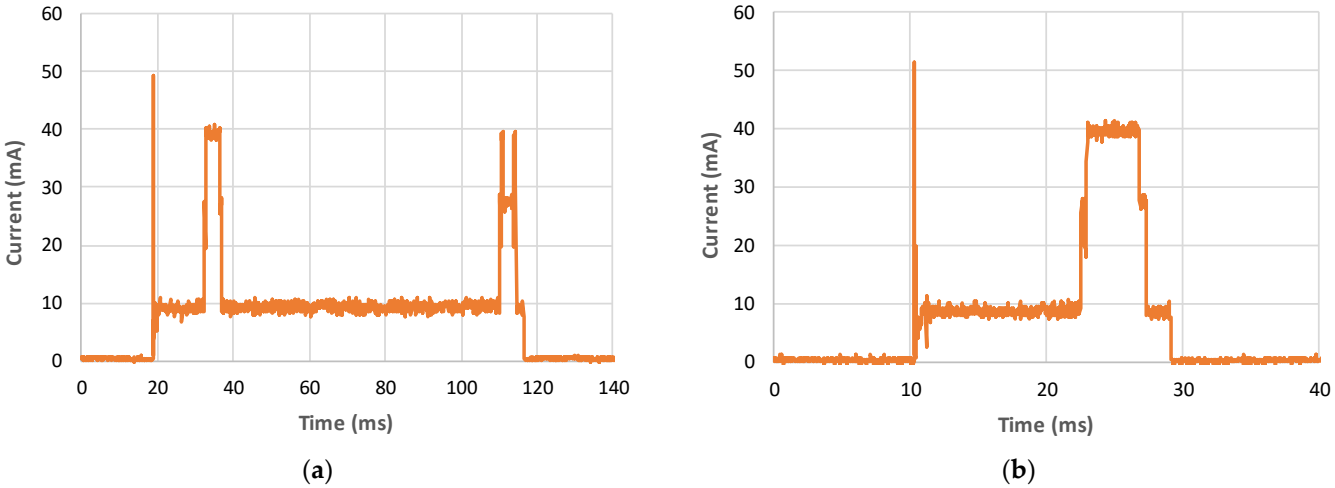

Figure 15. Current consumption: (**a**) with application ACK; (**b**) without application ACK.

The reduction in power consumption due to transmit power only occurs if the consumption of the control circuits of the directional antennas is less than that reduction. Electronically reconfigurable antennas are typically used to control the radiation pattern of directional antennas. The most common components employed in this control are

Positive–Intrinsic–Negative (PIN) diodes, Radio-Frequency Micro-Electromechanical Systems (RF MEMS) switches, and Varactors [12]. Most works prefer PIN diodes because they provide fast switching, ranging from 1 to 100 ns [41–43]. The current consumption of PIN diodes is in the range of 3 mA to 20 mA [12,44]. These values are higher than the increase in current consumption produced by omnidirectional antennas in the present study. RF MEMS represents another switching mechanism to control the radiation pattern. Their disadvantages are slow switching speed and high control voltage (20–100 V) [12,44]. Although the power consumption of these components is low, a DC–DC converter may be required to generate this voltage from a lower-voltage source. These converters tend to be very inefficient for low currents. Therefore, the current consumption of the complete circuit can be several milliamperes.

5. Conclusions

A study was carried out to evaluate the performance of directional antennas operating under NLOS conditions. As the work context was ZigBee networks, the power consumption of the transmission system must be low. Measurements with XBee radios operating at 2.4 GHz aimed to obtain the RSSI and PDR quality parameters. Three locations allowed the testing of different situations of NLOS propagation and Wi-Fi interference. We compared the performance of a directional antenna of 9.5 dBi with an omnidirectional antenna of 2 dBi. The transmission systems operated at the same EIRP. Although the directional antenna receiver had an additional 7.5 dB gain, the RSSI and PDR results were virtually the same for greater distances to the transmitter. To help understand this result, we applied a deconvolution technique to extract the received signal as a function of the azimuth angle. The results showed that the system with omnidirectional antennas performs better when receiving high-signal components from various angles. Directional antennas may also not prevent interference. The directional antenna received power from directions with high Wi-Fi interference in many measurement positions. Therefore, the directional antenna did not improve the SINR. The disadvantage of the omnidirectional antennas was to require a higher transmit power for the same range. The difference in current consumption between the highest and lowest power levels of the modules employed in the systems was less than three milliamperes. However, the study also demonstrated that the control circuits of directional antennas typically consume more than three milliamperes.

Directional antennas continue to be a good solution for increasing range in low-attenuation environments. Therefore, future work will investigate the performance implications of combining directional and omnidirectional antennas in ZigBee networks.

Author Contributions: Conceptualization, J.A.A.; methodology, J.A.A.; software, J.A.A. and F.E.S.; validation, J.A.A. and F.E.S.; formal analysis, J.A.A.; investigation, J.A.A.; resources, J.A.A. and F.E.S.; data curation, J.A.A.; writing—original draft preparation, J.A.A.; writing—review and editing, J.A.A. and F.E.S.; supervision, J.A.A.; project administration, J.A.A.; funding acquisition, J.A.A. All authors have read and agreed to the published version of the manuscript.

Funding: This research has been partially supported by the Center for Research in Mathematics and Applications (CIMA) related with the Statistics, Stochastic Processes and Applications (SSPA) group, through Project UIDB/04674/2020 of FCT—Fundação para a Ciência e a Tecnologia, Portugal.

Conflicts of Interest: The authors declare no conflict of interest.

References

1. Catarinucci, L.; Guglielmi, S.; Patrono, L.; Tarricone, L. Switched-beam antenna for wireless sensor network nodes. *Prog. Electromagn. Res. C* **2013**, *39*, 193–207. [CrossRef]
2. Curiac, D.I. Wireless sensor network security enhancement using directional antennas: State of the art and research challenges. *Sensors* **2016**, *16*, 488. [CrossRef] [PubMed]
3. Loh, T.H.; Lin, H. On the improvement of positioning accuracy in wireless sensor network using smart antennas. In Proceedings of the 2020 IEEE Eighth International Conference on Communications and Networking (ComNet), Hammamet, Tunisia, 27–30 October 2020. [CrossRef]

4. Ullah, M.A.; Keshavarz, R.; Abolhasan, M.; Lipman, J.; Esselle, K.P.; Shariati, N. A review on antenna technologies for ambient rf energy harvesting and wireless power transfer: Designs, challenges and applications. *IEEE Access* **2022**, *10*, 17231–17267. [CrossRef]
5. Prayati, A.; Antonopoulos, C.; Stoyanova, T.; Koulamas, C.; Papadopoulos, G. A modeling approach on the TelosB WSN platform power consumption. *J. Syst. Softw.* **2010**, *83*, 1355–1363. [CrossRef]
6. Catarinucci, L.; Guglielmi, S.; Collela, R.; Tarricone, L. Compact switched-beam antennas enabling novel power-efficient wireless sensor networks. *IEEE Sens. J.* **2014**, *14*, 3252–3259. [CrossRef]
7. Piyare, R.; Lee, S.R. Performance analysis of XBee ZB module based wireless sensor networks. *Int. J. Sci. Eng. Res.* **2013**, *4*, 1615–1621.
8. Dunlop, J.; Cortes, J. Impact of directional antennas in wireless sensor networks. In Proceedings of the 2007 IEEE International Conference on Mobile Adhoc and Sensor Systems, Pisa, Italy, 8–11 October 2007. [CrossRef]
9. Horvat, G.; Sostaric, D.; Žagar, D. Response surface methodology based power consumption and RF propagation analysis and optimization on XBee. *Telecommun. Syst.* **2015**, *59*, 437–452. [CrossRef]
10. Yabcznski, E.; Brante, G.; Souza, R.D.; Montejo-Sánchez, S. Energy efficient probabilistic switching on–off operation in multi-antenna cooperative wireless sensor networks. *Sensors* **2021**, *21*, 2937. [CrossRef]
11. George, R.; Mary, T.A.J. Review on directional antenna for wireless sensor network applications. *IET Commun.* **2020**, *14*, 715–722. [CrossRef]
12. Parchin, N.O.; Basherlou, H.J.; Al-Yasir, Y.I.A.; Abdulkhaleq, A.M.; Abd-Alhameed, R.A. Reconfigurable antennas: Switching techniques—A survey. *Electronics* **2020**, *9*, 336. [CrossRef]
13. Staniec, K.; Debita, G. Interference mitigation in WSN by means of directional antennas and duty cycle control. *Wirel. Commun. Mob. Comput.* **2012**, *12*, 1481–1492. [CrossRef]
14. Skiani, E.D.; Mitilineos, S.A.; Thomopoulos, S.C. A study of the performance of wireless sensor networks operating with smart antennas. *IEEE Antennas Propag. Mag.* **2012**, *54*, 50–67. [CrossRef]
15. Georgiou, O.; Wang, S.; Bocus, M.Z.; Dettmann, C.P.; Coon, J.P. Directional antennas improve the link-connectivity of interference limited ad hoc networks. In Proceedings of the 2015 IEEE 26th Annual International Symposium on Personal, Indoor, and Mobile Radio Communications (PIMRC), Hong Kong, China, 30 August–2 September 2007; pp. 1311–1316. [CrossRef]
16. Giorgetti, G.; Cidronali, A.; Gupta, S.K.S.; Manes, G. Exploiting low-cost directional antennas in 2.4 GHz IEEE 802.15.4 wireless sensor networks. In Proceedings of the 2007 European Conference on Wireless Technologies, Munich, Germany, 8–10 October 2007. [CrossRef]
17. Lin, S.; Miao, F.; Zhang, J.; Zhou, G.; Gu, L.; He, T.; Stankovic, J.A.; Son, S.; Pappas, G.J. ATPC: Adaptive transmission power control for wireless sensor networks. *ACM Trans. Sen. Netw.* **2016**, *12*, 16.1–36.1. [CrossRef]
18. Azevedo, J.A.R.; Sousa, T.A.; Santos, F.E.; Agrela, J.M. Impact of the antenna directivity on path loss for different propagation environments. *IET Microw. Antennas Propag.* **2015**, *9*, 1392–1398. [CrossRef]
19. Voigt, T.; Mottola, L.; Hewage, K. Understanding Link Dynamics in Wireless Sensor Networks with Dynamically Steerable Directional Antennas. In *Wireless Sensor Networks*; Lecture Notes in Computer Science; Demeester, P., Moerman, I., Terzis, A., Eds.; Springer: Berlin/Heidelberg, Germany, 2013; Volume 7772, pp. 115–130. [CrossRef]
20. Michalopoulou, A.; Koxias, E.; Lazarakis, F.; Zervos, T.; Alexandridis, A.A. Investigation of directional antennas effect on energy efficiency and reliability of the IEEE 802.15.4 standard in outdoor wireless sensor networks. In Proceedings of the 2015 IEEE 15th Mediterranean Microwave Symposium (MMS), Lecce, Italy, 30 November–2 December 2015. [CrossRef]
21. Felemban, E.; Murawski, R.; Ekici, E.; Park, S.; Lee, K.; Park, J.; Hameed, Z. SAND: Sectored-antenna neighbor discovery protocol for wireless networks. In Proceedings of the 2010 7th Annual IEEE Communications Society Conference on Sensor, Mesh and Ad Hoc Communications and Networks (SECON), Boston, MA, USA, 21–25 June 2010. [CrossRef]
22. Chen, Y.C.; Wen, C.Y. Distributed clustering with directional antennas for wireless sensor networks. *IEEE Sens. J.* **2013**, *13*, 2166–2180. [CrossRef]
23. Yu, Z.; Teng, J.; Bai, X.; Xuan, D.; Jia, W. Connected coverage in wireless networks with directional antennas. *ACM Trans. Sens. Netw.* **2014**, *10*, 51.1–51.28. [CrossRef]
24. Nilsson, M. Directional antennas for wireless sensor networks. In Proceedings of the of the 9th Scandinavian Workshop on Wireless Adhoc Networks (Adhoc'09), Uppsala, Sweden, 4–5 May 2009.
25. Liang, B.; Sanz-Izquierdo, B.; Batchelor, J.C.; Bogliolo, A. Active FSS enclosed beam-switching node for wireless sensor networks. In Proceedings of the 8th European Conference on Antennas and Propagation (EuCAP 2014), Hague, The Netherlands, 6–11 April 2014. [CrossRef]
26. Wang, R.; Wang, B.Z.; Huang, W.Y.; Ding, X. Compact reconfigurable antenna with an omnidirectional pattern and four directional patterns for wireless sensor systems. *Sensors* **2016**, *16*, 552. [CrossRef]
27. Dao, H.N.; Krairiksh, M.; Le, D.T. A design of switched-beam Yagi-Uda antenna for wireless sensor networks. In Proceedings of the 2016 International Conference on Advanced Technologies for Communications (ATC), Hanoi, Vietnam, 12–14 October 2016. [CrossRef]
28. Dihissou, A.A.N.; Diallo, A.; Thuc, P.L.; Staraj, R. Directive and reconfigurable antenna for wireless sensor network to improve link quality between nodes. In Proceedings of the 2019 IEEE Sensors Applications Symposium (SAS), Sophia Antipolis, France, 11–13 March 2019. [CrossRef]

29. Rahman, M.; NagshvarianJahromi, M.; Mirjavadi, S.S.; Hamouda, A.M. Compact UWB band-notched antenna with integrated bluetooth for personal wireless communication and UWB applications. *Electronics* **2019**, *8*, 158. [CrossRef]
30. Nagaraju, S.; Gudino, L.; Kadam, B.; Khairnar, V.V.; Rodrigues, J.X.; Ramesha, C.K. Rectangular microstrip patch antenna array based sectored antenna for directional wireless sensor networks. In Proceedings of the 2020 12th International Symposium on Communication Systems, Networks and Digital Signal Processing (CSNDSP), Porto, Portugal, 20–22 July 2020. [CrossRef]
31. Surier, A.; Leingthone, M.M.; Hakem, N.; Mission, M. Adapted low-footprint biasing circuit for switched beam antenna steering usable in wireless sensor networks. In Proceedings of the 2020 14th European Conference on Antennas and Propagation (EuCAP), Copenhagen, Denmark, 15–20 March 2020. [CrossRef]
32. Oliveira, T.E.S.; Reis, J.R.; Vala, M.; Caldeirinha, R.F.S. High performance antennas for early fire detection wireless sensor networks at 2.4 GHz. In Proceedings of the 2021 IEEE-APS Topical Conference on Antennas and Propagation in Wireless Communications (APWC), Honolulu, HI, USA, 9–13 August 2021. [CrossRef]
33. Gahgouh, S.; Saidi, I.; Gharsallah, A. Slotted cubic design for 2.4 GHZ antenna. In Proceedings of the 2022 5th International Conference on Advanced Systems and Emergent Technologies (IC_ASET), Hammamet, Tunisia, 22–25 March 2022. [CrossRef]
34. Digi. Available online: https://www.digi.com (accessed on 7 April 2022).
35. Laird Connectivity. Available online: https://www.lairdconnect.com/documentation/24-ghz-dipole-antenna-datasheet (accessed on 1 May 2022).
36. Cui, H.; Caldeirinha, R.; Richter, J. A deconvolution method to remove distortion caused by antenna radiation pattern from measurement. In Proceedings of the 2010 International Workshop on Antenna Technology (iWAT), Lisbon, Portugal, 1–3 May 2010. [CrossRef]
37. Dhaene, T.; Martens, Z.; De Zutter, D. Extended bennia-riad criterion for iterative frequency-domain deconvolution. *IEEE Trans. Instrum. Meas.* **1994**, *43*, 176–180. [CrossRef]
38. Vaunix Technology Corporation. Available online: https://vaunix.com/lsg-602-digital-signal-generator (accessed on 7 April 2022).
39. Rohde & Schwarz. Available online: https://www.rohde-schwarz.com/us/products/test-and-measurement/handheld/rs-fsh-handheld-spectrum-analyzer_63493-8180.html (accessed on 7 April 2022).
40. Song, J.; Tan, Y.K. Energy consumption analysis of ZigBee-based energy harvesting wireless sensor networks. In Proceedings of the 2012 IEEE International Conference on Communication Systems (ICCS), Singapore, 21–23 November 2012. [CrossRef]
41. Gu, C.; Gao, S.; Liu, H.; Lou, Q.; Loh, T.H.; Sobhy, M.; Li, J.; Wei, G.; Xu, J.; Qin, F.; et al. Compact smart antenna with electronic beam-switching and reconfigurable polarizations. *IEEE Trans. Antennas Propag.* **2015**, *63*, 5325–5333. [CrossRef]
42. Lu, Z.L.; Yang, X.X.; Tan, G.N. A multidirectional pattern-reconfigurable patch antenna with CSRR on the ground. *IEEE Antennas Wirel. Propag. Lett.* **2017**, *16*, 416–419. [CrossRef]
43. Parchin, N.O.; Basherlou, H.J.; Al-Yasir, Y.I.A.; Abd-Alhameed, R.A.; Abdulkhaleq, A.M.; Noras, J.M. Recent developments of reconfigurable antennas for current and future wireless communication systems. *Electronics* **2019**, *8*, 128. [CrossRef]
44. Christodoulou, C.G.; Tawk, Y.; Lane, S.A.; Erwin, S.R. Reconfigurable antennas for wireless and space application. *Proc. IEEE* **2012**, *100*, 2250–2261. [CrossRef]